https://doi.org/10.1016/j.matlet.2017.11.033

Magnetotransport properties of $Ca_{0.8}La_{0.2}IrO_3$ epitaxial films

Y. K. Liu, H.F. Wong, S.M. Ng, K.K. Lam, C.L. Mak and C.W. Leung*

Department of Applied Physics, The Hong Kong Polytechnic University, Hung Hom, Hong Kong, China

Abstract

We fabricated high-quality epitaxial $Ca_{0.8}La_{0.2}IrO_3$ (CLIO) films on $SrTiO_3$ (STO), $(LaAlO_3)_{0.3}(Sr_2AlTaO_6)_{0.7}$ (LSAT) and $NdGaO_3$ (NGO) substrates by pulsed laser deposition, and systematically studied their transport properties. All samples showed insulating behavior, but the resistivity of CLIO/NGO film showed relatively weak temperature dependence and can be regarded as a poor metallic behavior. The carrier transport in all the samples were dominated by the Mott-type variable range hopping. The magnetoresistance of CLIO/NGO showed a value about 6%, larger than that of CLIO/STO and CLIO/LSAT, while the CLIO/STO sample showed very large magnetic moment and small coercive field. These findings indicate that mechanical strain can be a useful route to explore the unusual physics of iridates with strong spin-orbit coupling.

Keywords: spin-orbital coupling; iridates; epitaxial thin films; magnetoresistance.

* Electronic mail: dennis.leung@polyu.edu.hk

Introduction

Over the past few decades, transition-metal perovskite oxides ABO_3 with strong electronic correlations have attracted considerable attention, due to various unconventional physical phenomena and significant potential applications, such as colossal magnetoresistance[1], high temperature superconductivity[2], ferroelectric [3] and multiferroic properties[4, 5]. Currently, there is a strong interest to explore novel electronic and magnetic phases in 5*d* transition metal iridates with larger spin-orbit-coupling (SOC), which are related to the exotic behavior such as Weyl semimetals [6], quantum spin Hall effect [7], topological properties [8], and possible superconductivity with *d*-wave gap[9].

Most studies to date concerning iridates focused on the Ruddlesden-Popper phases of $Sr_{n+1}Ir_nO_{3n+1}$ (n=1, 2, ⋯, ∞)[10-13], and one of the most interesting research is to search for metal-insulator transition or even superconductivity by 20% La doping [14, 15]. Recently, Ohgushi *et al*. confirmed $CaIrO_3$ also exhibited a Mott insulator behavior with J_{eff} = 1/2 state by resonant x-ray diffraction [16]. The smaller ionic size of Ca^{2+} compared to Sr^{2+} resulted in increased IrO_6 octahedral rotation and hence a reduced electronic bandwidth [17]. Thus, it is expected that the strength of spin-orbit coupling in $CaIrO_3$ films can be manipulated by tailoring substrate-induced epitaxial strain [18, 19].

In this letter, we fabricated epitaxial $Ca_{0.8}La_{0.2}IrO_3$ (CLIO) films on $SrTiO_3$ (STO), $(LaAlO_3)_{0.3}(Sr_2AlTaO_6)_{0.7}$ (LSAT) and $NdGaO_3$ (NGO) substrates by pulsed laser deposition and investigated their transport properties. There were previous studies on the strain dependence of transport and magnetic properties in $SrIrO_3$, Sr_2IrO_4 and $CaIrO_3$ films [19-21] , but to our knowledge CLIO films were

not investigated for similar behavior so far. The resistivity of these films showed insulating behavior and can be fitted by the Mott variable range hopping mechanism. Importantly, the CLIO/NGO sample exhibited the largest magnetoresistance (MR) and underwent a negative-to-positive MR transition with increasing temperature. The weak FM behavior in CLIO/STO film with larger magnetic moment and smaller coercive field may come with strain-induced variation of Ir-O/Ir-Ir bond lengths. Our results demonstrate that strain plays a key role in manipulating the transport properties of iridates.

Experiment

A series of epitaxial CLIO films (45 nm) were deposited on STO (001), LSAT (001) and NGO (110) substrates by pulsed laser deposition with laser wavelength of 248 nm. Polycrystalline CLIO target was prepared by conventional solid-state reaction. Laser fluence and repetition rate were ~1.5 J-cm^{-2} and 1 Hz, respectively. During deposition, the substrates temperature was kept at 710˚C and the oxygen pressure was 200 mTorr, and the target-to-substrate distance was 5 cm. After the deposition, the films were annealed at 10 Torr of oxygen and then cooled down naturally to room temperature.

The crystallographic structure of the samples was characterized using X-ray diffraction (XRD) measurement (SmartLab, Rigaku Co.) with Cu $K_{\alpha 1}$ radiation (λ_{XRD} = 1.5406 Å). The transport properties were measured using a Physical Property Measurement System (PPMS, Quantum Design Co.).

Results and discussions

Fig. 1 shows the x-ray θ-2θ scans of epitaxial CLIO films grown on different substrates, indicating single-phased (00*l*)-oriented perovskite CLIO reflections with no trace of impurities or additional phases. The reported pseudo-cubic lattice parameter (a_{pc}) of the perovskite $CaIrO_3$ bulk is a_{pc} ~ 3.855Å [22], and the lattice parameters of NGO, LSAT and STO are 3.861 Å, 3.868 Å and 3.905 Å, respectively. It is worth noting that the replacement of Ca ions (1.0 Å) by La (1.032 Å) will slightly increase the lattice parameter and affects the distortion angle of the IrO_6 octahedra, which can influence the transport properties of the films [17]. Inset of Fig.1 shows the relation between the substrate lattice and film out-plane lattice *c*, indicating *c* increases with rising substrate lattice constant.

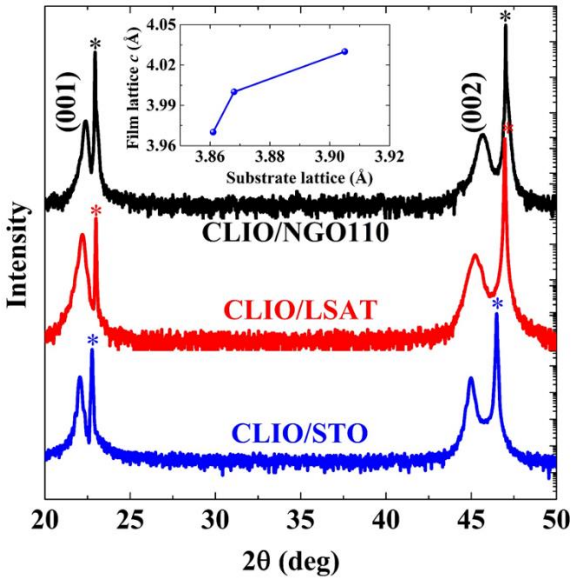

Fig. 1. X-ray diffraction patterns of CLIO films grown on different substrates. Inset shows the relation between film lattice and substrates lattice. The substrate peaks are marked by asterisks.

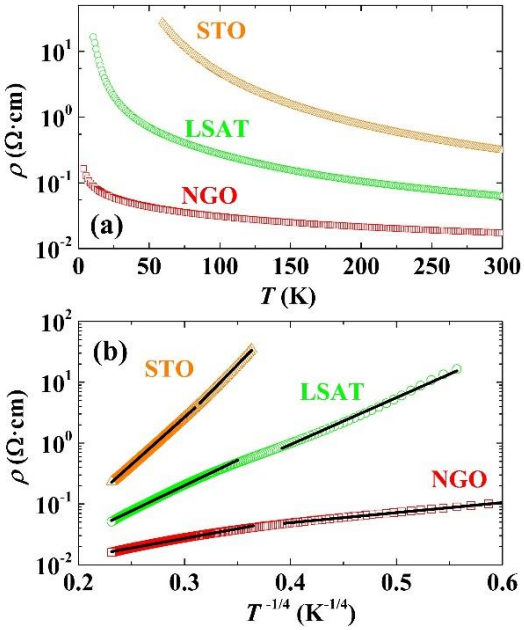

Fig. 2. (a) Temperature dependence of the resistivity of CLIO films grown on different substrates. (b) Resistivity of the data in (a) as a function of $T^{-1/4}$. Solid lines are fittings based on the 3D Mott-VRH model.

The temperature dependence of CLIO film resistivity $\rho(T)$ is shown in Fig. 2(a). All the samples show insulating behavior in the whole temperature range measured, which is consistent with the reported Mott insulating state of the $CaIrO_3$ in film [18, 19] and bulk forms [23]. At 300 K, CLIO/NGO sample shows the smallest resistivity (ρ) about 15 mΩ·cm, which is a slightly larger than that of $CaIrO_3$/NGO (4 mΩ·cm) [18]. Compared to CLIO/LSAT and CLIO/STO films, the temperature dependence of ρ for the CLIO/NGO sample is quite weak. As for the CLIO/LSAT sample, the resistivity ratio (ρ_{10K}/ρ_{300K}) can reach about 260 which is much larger than that of $CaIrO_3$/LSAT film [19]. The resistivity of CLIO/STO sample gets much more sensitive to temperature variation, with its resistivity that is beyond our measurement limit at ~ 50 K. The resistivity ratio of CLIO/NGO and CLIO/STO can reach up to the order of 10^2, indicating the significant effect of strain. The different dependence of $\rho(T)$ curves on substrate was reported in other iridates with

larger SOC such as Sr_2IrO_4 [21], $Sr_{1.8}La_{0.2}IrO_4$ [24], and $SrIrO_3$ [20], which is induced by the strain-induced the variation of IrO_6 octahedral distortion. The robust insulating behavior of CLIO under strain may originate from the symmetry-protected Dirac nodes due to a combined effect of SOC and lattice distortion [19, 21].

Recently, a conduction mechanism for SOC-induced Mott insulators was reported in iridates oxides [25, 26], where the transport behavior can be fitted by the 3-dimensional Mott variable range hopping (3D Mott-VRH) mechanism $\rho=\rho_0 exp[(T_M/T)^{1/4}]$. Here, ρ_0 is the resistivity coefficient and T_M is the characteristic temperature which is closely related to the density of state and the localization length. The fitted results are shown in Fig. 2(b), where $ln\,\rho \propto T^{-1/4}$ shows very good linear behavior with different slopes at two distinct temperature ranges, suggesting two distinct values of T_M (T_{M1} for high-T, and T_{M2} for low-T). The fitted parameters of T_{M1} are 2.82×10^3K, 1.38×10^5K, and 1.64×10^6K, and T_{M2} are 207K, 1.0×10^5K, and 2.81×10^6K, for CLIO films grown on NGO, LSAT and STO substrates, respectively. These values are comparable to those obtained in Sr_2IrO_4 film [27]. Note that the characteristic temperatures T_{M1} and T_{M2} show a difference of three orders of magnitude for various substrates, suggesting the significant impact of strain on the transport properties by modifying the band structure of CLIO film [20].

Fig. 3 exhibits the magnetoresistance (MR) effect of CLIO films at different temperatures and with applied magnetic field up to 9 T. Here, MR is defined as $[\rho(H) - \rho(0)]/\rho(0)$, where $\rho(0)$ and $\rho(H)$ are the resistivities of the samples without and with external applied magnetic field, respectively. At 5 K the CLIO/NGO film shows a negative MR (Fig. 3(a)) of 6% at 9 T, which can be attributed to magnetic

field suppressing the spin-dependent scattering. The magnitude of MR decreases with increasing *T*, due to increasing spin-dependent scattering and larger thermal fluctuations with increasing *T*. A sign change of MR ratio occurs at 50 K, and no MR can be measured beyond 100 K. The reversal in MR has been reported in $SrIrO_3$ [20] and Sr_2IrO_4 films [21, 28], in which the negative MR was attributed to the spin-dependent scattering mechanism while the magnetoelastic effect was suggested to be responsible for the positive MR. As for the CLIO/LSAT film (Fig. 3(b)), the MR behavior is similar with that in CLIO/NGO sample except for a slightly smaller MR, and CLIO/STO film shows the smallest MR among all samples studied (Fig. 3(c)). The MR of CLIO/NGO sample is about one order larger than that of CLIO/STO, similar to the reported in $SrIrO_3$ film[20], resulting from the rotation of oxygen octahedra, which further evidenced the strain plays a significant role in the magnetotransport properties.

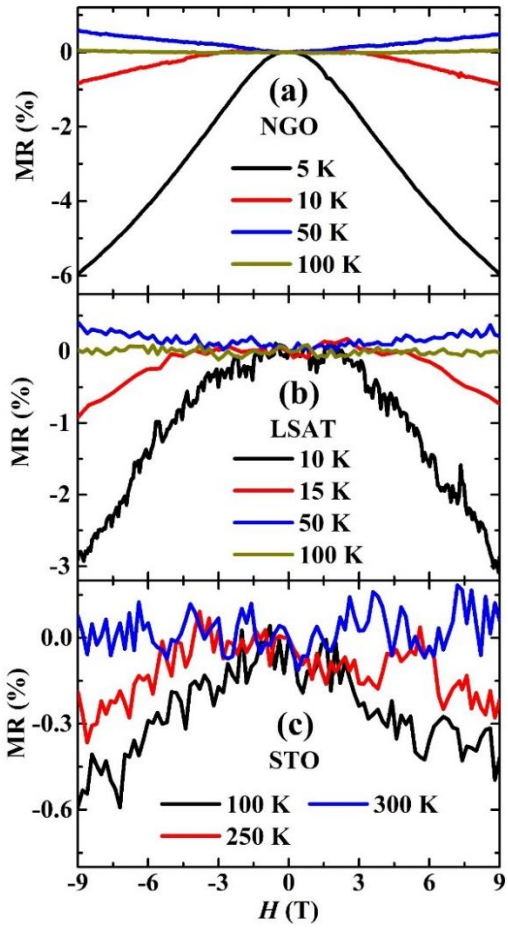

Fig. 3. Magnetoresistance of CLIO films grown on NGO (a), LSAT (b), and STO (c) substrates.

Fig. 4 shows the magnetic properties of CLIO films grown on LSAT and STO substrates. Due to the strong diamagnetic response of NGO, it is difficult to separate the genuine CLIO magnetic moment from that of the NGO substrates［21, 29］. Actually perovskite $CaIrO_3$ system exhibits Pauli paramagnetic characteristics［22, 23］. Based on the above results and discussions, it is expected that the strain should have an effect on the magnetic properties of CLIO. From the temperature dependence of magnetization (*M*-*T*) curves (Fig. 4(a)) and magnetic hysteresis loops at 5 K (Fig. 4(b)), it is obvious that the magnetic moment of CLIO/STO is much larger than that of CLIO/LSAT sample, and the coercive field of CLIO/STO

is much smaller than that of CLIO/LSAT sample. The enhanced moment in CLIO/STO sample can be understood by considering the strain-induced variation of Ir-O/Ir-Ir bond lengths, yielding a nonzero net moment [30]. Based on above our transport and magnetic measurement results of CLIO films on different substrates, it can be concluded that the physical properties of CLIO film are closely related to the epitaxial strain, which induces the variation of IrO_6 octahedral and change the Ir-O/Ir-Ir bond lengths or the bandwidth [20, 31].

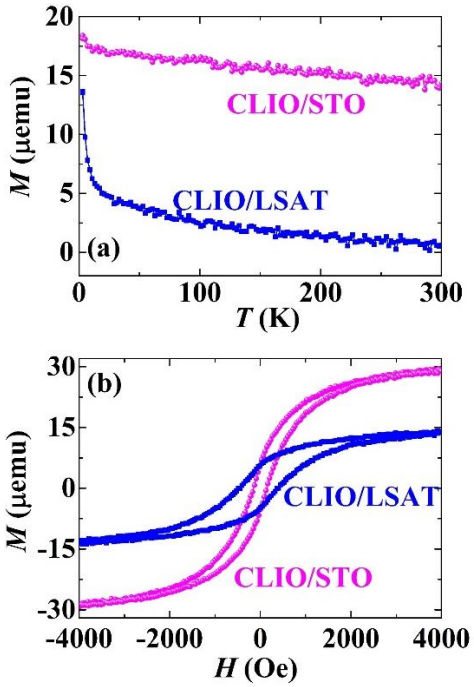

Fig. 4. Temperature dependence of magnetization (a) and magnetic hysteresis loops (b) of CLIO films grown on LSAT and STO substrates.

Conclusion

In conclusion, the structural and transport properties of epitaxial $Ca_{0.8}La_{0.2}IrO_3$ films grown on STO, LSAT and NGO substrates are investigated. The conduction behavior in the samples could be explained by the Mott variable range hopping model. Among the samples studied, CLIO/NGO sample showed a weak temperature dependence of resistivity but the largest magnetoresistance, and the magnetoresistance can undergo a sign change from negative to positive with increasing temperature. As is well known that in 5*d* iridates the energy scale of spin-orbit coupling is typically comparable to that of the Coulomb interaction. Thus the structure (IrO_6 distortion) impact would have significant influence on the transport and magnetic properties of the epitaxial films as demonstrated in this work, and our results suggest that strain will be one promising route to tune the physical properties of iridates.

Acknowledgement

Y.K. Liu acknowledges the financial support from the National Natural Science Foundation of China (Grant No.51502129). C.W. Leung acknowledges the financial support from UGC, HKSAR (PolyU 153015/14 P) and PolyU (1-ZE25, 1-ZVGH).

References:

[1] M. B. Salamon and M. Jaime, Reviews of Morden of Physics 73 (2001) 583.
[2] N. P. Armitage, P. Fournier, and R. L. Greene, Rev. Mod. Phys. 82 (2010) 2421.
[3] M. Dawber, K. M. Rabe, and J. F. Scott, Rev. Mod. Phys. 77 (2005) 1083.
[4] R. Ramesh, Philos Trans A Math Phys Eng Sci 372 (2014) 20120437.
[5] J. T. Heron, et al., Nature 516 (2014) 370.
[6] P. Hosur, S. A. Parameswaran, and A. Vishwanath, Phys. Rev. Lett. 108 (2012) 046602.
[7] A. Shitade, H. Katsura, J. Kunes, X. L. Qi, S. C. Zhang, and N. Nagaosa, Phys. Rev. Lett. 102 (2009) 256403.
[8] Y. Chen, Y. M. Lu, and H. Y. Kee, Nat Commun 6 (2015) 6593.
[9] Y. K. Kim, N. H. Sung, J. D. Denlinger, and B. J. Kim, Nat. Phys. 12 (2016) 37.
[10] S. J. Moon, et al., Phys. Rev. Lett. 101 (2008) 226402.
[11] B. J. Kim, H. Ohsumi, T. Komesu, S. Sakai, T. Morita, H. Takagi, and T. Arima, Science 323 (2009) 1329.
[12] P. E. R. Blanchard, E. Reynolds, B. J. Kennedy, J. A. Kimpton, M. Avdeev, and A. A. Belik, Phys. Rev. B 89 (2014) 214106
[13] M. Miyazaki, R. Kadono, M. Hiraishi, A. Koda, K. M. Kojima, K. Ohashi, T. Takayama, and H. Takagi, Phys. Rev. B 91 (2015) 155113.
[14] F. Wang and T. Senthil, Phys. Rev. Lett. 106 (2011) 136402.
[15] Y. Gao, T. Zhou, H. Huang, and Q. H. Wang, Scientific reports 5 (2015) 9251.
[16] K. Ohgushi, J. Yamaura, H. Ohsumi, K. Sugimoto, S. Takeshita, A. Tokuda, H. Takagi, M. Takata, and T. H. Arima, Phys Rev Lett 110 (2013) 217212.
[17] S. Y. Jang, H. Kim, S. J. Moon, W. S. Choi, B. C. Jeon, J. Yu, and T. W. Noh, Journal of physics. Condensed matter : an Institute of Physics journal 22 (2010) 485602.
[18] A. Biswas and Y. H. Jeong, J. Appl. Phys. 117 (2015) 195305.
[19] D. Hirai, J. Matsuno, D. Nishio-Hamane, and H. Takagi, Appl. Phys. Lett. 107 (2015) 012104.
[20] J. H. Gruenewald, J. Nichols, J. Terzic, G. Cao, J. W. Brill, and S. S. A. Seo, J. Mater. Res. 29 (2014) 2491.
[21] L. Miao, H. Xu, and Z. Q. Mao, Phys. Rev. B 89 (2014) 035109.
[22] J. G. Cheng, J. S. Zhou, J. B. Goodenough, Y. Sui, Y. Ren, and M. R. Suchomel, Phys. Rev. B 83 (2011) 064401.
[23] K. Ohgushi, T. Yagi, H. Gotou, Y. Kiuchi, and Y. Ueda, Physica B: Condensed Matter 404 (2009) 3261.
[24] M. Ito, M. Uchida, Y. Kozuka, K. S. Takahashi, and M. Kawasaki, Phys. Rev. B 93 (2016)
[25] G. Cao, J. Bolivar, S. McCall, J. E. Crow, and R. P. Guertin, Phys. Rev. B 57 (1998) R11039.
[26] O. B. Korneta, T. Qi, S. Chikara, S. Parkin, L. E. De Long, P. Schlottmann, and G. Cao, Phys. Rev. B 82 (2010)
[27] C. Lu, A. Quindeau, H. Deniz, D. Preziosi, D. Hesse, and M. Alexe, Appl. Phys. Lett. 105 (2014) 082407.
[28] C. Lu, S. Dong, A. Quindeau, D. Preziosi, N. Hu, and M. Alexe, Phys. Rev. B 91 (2015) 104401.
[29] J. Dho, Y. N. Kim, Y. S. Hwang, J. C. Kim, and N. H. Hur, Appl. Phys. Lett. 82 (2003) 1434.
[30] A. Lupascu, et al., Phys Rev Lett 112 (2014) 147201.
[31] A. Biswas, K.-S. Kim, and Y. H. Jeong, J. Appl. Phys. 116 (2014) 213704.